

Rapid Communication

Biferroic YCrO₃

Claudy Rayan Serrao^{1,2}, Asish K. Kundu¹, S. B. Krupanidhi², Umesh V. Waghmare^{1,3},
and C. N. R. Rao^{1,2*}

¹*Chemistry and Physics of Materials Unit, Jawaharlal Nehru Centre for Advanced
Scientific Research, Bangalore –560064, India.*

²*Material Research Centre, Indian Institute of Science, Bangalore-560012, India.*

³*Theoretical Sciences Unit, Jawaharlal Nehru Centre for Advanced Scientific Research,
Bangalore –560064, India.*

PACS numbers:

71.15.-m 71.20.-b 71.23.An 75.50.-y 75.60.-d 77.22.-d 77.55.+f 77.80.-e 81.15.Fg

Abstract:

YCrO₃ which has a monoclinic structure, shows weak ferromagnetism below 140 K (T_N) and a ferroelectric transition at 473 K accompanied by hysteresis. We have determined the structure and energetics of YCrO₃ with ferromagnetic and antiferromagnetic ordering by means of first-principles density functional theory calculations, based on pseudopotentials and a plane wave basis. The non-centrosymmetric monoclinic structure is found to be lower in energy than the orthorhombic structure, supporting the biferroic nature of YCrO₃.

*Corresponding author: cnrao@jncasr.ac.in

There has been much interest in biferroic materials in recent years.¹⁻⁴ Research in this field is of great interest because of the potential uses of materials with simultaneous ferroelectric and magnetic orderings. Some of these materials exhibit a ferroelectric transition at a relatively high temperature and a magnetic transition at a lower temperature. One such material in this category is BiMnO₃ with the ferroelectric transition (T_E) at 450 K and the ferromagnetic transition around (T_C) 105 K.^{5,6} BiFeO₃, on the other hand, exhibits a T_E of 1110 K and an antiferromagnetic transition (T_N) at 670 K.⁷ BiCrO₃ is recently reported to exhibit a T_E of 440 K and T_N of 114 K.⁸ Unlike these materials, TbMnO₃ shows a different behavior, wherein T_E is lower than the T_C ; here, the spin frustration causes the ferroelectric distortion. In addition to BiMnO₃, hexagonal rare earth manganates LnMnO₃ (with Ln = Ho, Er, Tm, Yb, Lu or Y) are known to be biferroic with $T_E \gg T_N$.⁹ Thus, YMnO₃ is ferroelectric around 914 K and antiferromagnetic at 80 K.¹⁰ Considering that BiCrO₃ is biferroic just like BiMnO₃, it occurred to us that rare earth chromites such as YCrO₃ may exhibit interesting biferroic properties, a view somewhat strengthened by the suspected ferroelectricity in some of them.¹¹

Careful powder diffraction studies show that YCrO₃ has a monoclinic structure, as reported in the literature,¹² but the Rietveld analysis could not clearly distinguish between the centrosymmetric and non-centrosymmetric structures. However, our first-principles study (discussed later in the article) has shown the non-centrosymmetric structure to be energetically more stable. YCrO₃ is an antiferromagnet with weak ferromagnetism ($T_N = 140$ K).^{13,14} Our magnetic measurements show an increase in the magnetization around

140 K and the presence of magnetic hysteresis below this temperature (Fig. 1). Clearly, YCrO_3 exhibits features similar to those of a canted antiferromagnetic system.

We have investigated the dielectric properties of pressed pellets as well as thin films of YCrO_3 . The thin films were deposited using a KrF excimer laser of 248nm (λ physik) at 650°C in an oxygen ambient of 100mTorr with pulse energy of 140mJ/pulse on $\langle 111 \rangle$ oriented Pt/TiO₂/SiO₂/Si substrates. The dielectric phase transition observed in a YCrO_3 pellet is shown in Figure 2(a). The transition occurs over the 410-440 K range with a maximum (T_{max}) of 418K at 500Hz. The T_{max} is frequency dependent. The Curie Weiss plot of $1/\epsilon$ vs T gives a T_C of 473 K which is frequency independent as expected of a ferroelectric material.¹⁵ The dielectric constant shows a large dispersion below T_C , but is frequency-independent above T_C , a behavior commonly observed in relaxor ferroelectrics.¹⁶ The room-temperature dielectric constant is around 8000 at 5 kHz. A broad transition in normal ferroelectrics is attributed due to the presence of fine grains and the relaxor-like behavior may not be the property of the parent material itself. The presence of charged oxygen vacancies and the short range polar regions can, however, give rise to a relaxor like behavior in a normal ferroelectric.¹⁷ The role of oxygen vacancies and the presence of nanopolar regions and their role in the relaxor-like behavior in YCrO_3 is under study.

Studies of the YCrO_3 thin films, show a dielectric phase transition around 400K at 500 Hz as can be seen from Fig. 2(b). The monotonous increase in the dielectric constant at low frequencies above the T_C is associated with the dc conduction. Accordingly, we observe high dissipation factors of 2.348 and 38.834 (5 kHz) at room temperature in the bulk sample and the thin film respectively. The high-temperature loss shows a

monotonous rise due to the increase in the dc leakage current at high temperatures, and efforts are in progress to minimize the losses through processing. The dielectric phase transition found both in the pellets and the thin films also lends evidence for the presence of a ferroelectric phase in YCrO_3 .

The ferroelectric behavior of the YCrO_3 pellets and films was also confirmed by their room temperature capacitance-voltage (C-V) characteristics. The butterfly nature of the CV curves [Fig. 3(a)] suggests a weak ferroelectric behavior at room temperature.¹⁸ The room-temperature polarization-electric field (P-E) measurements on the pellets and thin films of YCrO_3 show the presence of hysteresis. We show hysteresis curves at different temperatures in Fig. 3(b). The maximum polarization observed is $2 \mu\text{C}/\text{cm}^2$ at 300 K in the case of the pellet and $3 \mu\text{C}/\text{cm}^2$ at 178K in the case of the thin film. Clearly, YCrO_3 exhibits a weak ferroelectric behavior from T_E to low temperatures through the magnetic transition.

Based on measurements of the X-ray powder diffraction data, $P2_1/n$ (space group no.14) has been suggested as a probable space group for YCrO_3 in the literature.¹² As $P2_1/n$ is a centrosymmetric monoclinic space group, our finding of ferroelectricity in YCrO_3 needs an explanation. To this end, we have carried out first-principles spin dependent density functional theory calculations using a standard plane-wave code PWSCF 2.0.1¹⁹ with a generalized gradient approximation²⁰ to the interaction energy of electrons. We used ultra-soft pseudo-potentials²¹ to represent the interaction between the ions and the electrons and treated semi-core s and p states of Y and Cr explicitly. An energy cutoff of 30 Ry (180 Ry) on the plane wave basis was used in representation of wave-functions (density). Most calculations involved unit cells with 40 and 20 atoms, and

Brillouin zones integrations were sampled with a Monkhorst-Pack mesh of k -points that is equivalent to a $4 \times 4 \times 4$ uniform mesh²² in the Brillouin zone of a crystal with 5 atoms per cell. In all calculations, we used experimental lattice parameters or volume of unit cell.²³

As $P2_1/n$ is a relatively low-symmetry space group, determination of the YCrO_3 structure with many structural parameters becomes challenging. We followed two procedures: (a) We first optimized the structure with a constraint of $P2_1/n$ symmetry. A further relaxation was carried out by breaking its inversion symmetry through off-centering of Y and Cr atoms. (b) We started with an initial structure obtained by randomly off-centering various atoms in the perovskite unit cell, and relaxed the structure to minimize energy. Structural optimization was first carried out maintaining a G -type antiferromagnetic ordering, and it was reassuring to find essentially the same final structure (Fig. 4) with both the procedures. The final structure has a broken inversion symmetry, supporting the possibility of ferroelectricity in YCrO_3 . From the procedure (a), we find that the final AFM structure is indeed lower in energy than the relaxed centrosymmetric $P2_1/n$ phase by 0.025 eV/formula unit. Our guess for the space group of the lowest energy structure of YCrO_3 is the monoclinic $P2_1$ (no. 4), though we find tiny distortions of the structure that amount to further lowering of symmetry. In this distorted perovskite structure, the average oxygen coordination of Y is about 6. Structural distortions of the parent cubic perovskite structure leading to the ferroelectric structure [shown in Figure 4(a)] have been analyzed by writing them as a linear combination of normal modes of the cubic structure. For YCrO_3 , we find the largest component of structural distortions to be associated with (a) M_3 modes [$k = (011) \pi/a$], (b) R_{25} modes [k

= (111) π/a], which correspond to rotations of oxygen octahedral, and (c) M_5 modes. There is a small component of modes with Y and oxygen displacements such as X_5' , R_{15} and Γ_{15} modes. There are no structural distortions with Cr displacements. The modes in (a) and (b) dominating the low-temperature phase do not break the inversion symmetry, while the relatively weak distortions of the mode Γ_{15} give rise to ferroelectricity.

Using the relaxed structure with AFM ordering as an initial guess, we optimized the structure of $YCrO_3$ with ferromagnetic ordering. While the relaxed structure with ferromagnetic ordering also exhibits a broken inversion symmetry, it is higher in energy than the structure with G -AFM ordering by about 0.04 eV/formula unit. For both types of ordering, the self-consistently determined local magnetic moment at Cr site is close to 3 μ_B consistent with fully occupied t_{2g} states of Cr just below the energy gap, as seen in the densities of electronic states (shown in Fig. 5). This results in a spin density with almost cubic symmetry centered at the Cr sites [see Fig. 4(b)]. Unlike many other materials, $YCrO_3$ is insulating in both FM and AFM ordered states with an energy gap of 1.3 eV and 1.8 eV respectively, and exhibits a large exchange splitting. We used the Berry phase²⁴ method to compute polarization and find P along a-axis to be about 3 $\mu C/cm^2$.

To understand the origin of ferroelectricity in $YCrO_3$ we studied the structural instabilities in the cubic perovskite structure of $YCrO_3$. We used a unit cell doubled along the $\langle 111 \rangle$ direction with a G -type AFM ordering and determined phonon frequencies at its Γ point, which correspond to phonons at Γ and R (folded for the supercell) points of the single perovskite unit cell. We find two triply degenerate instabilities, the strongest one (about 300 cm^{-1}) exhibits rotational motion of oxygen octahedra, and a weaker instability (about 100 cm^{-1}) of Y displacements with respect to oxygen cage. Note that the

former gives an anti-ferrodistortive phase while the latter is responsible for a ferroelectric phase. To probe anharmonic strength of the ferroelectric instability, we distorted the structure by freezing in Y displacements and relaxed it maintaining a rhombohedral symmetry and *G*-AFM ordering. We find an energy lowering by 0.089 eV/formula unit, comparable to other perovskite ferroelectrics like PbTiO_3 .²⁵ Interestingly, for a rhombohedral symmetry and FM ordering, optimized ferroelectric structure is lower than the paraelectric structure by 0.13 eV/formula unit, though is higher in energy than the ferroelectric structure with AFM ordering. In both FM and AFM ordering, off-centering of Cr atoms is not favored energetically.

In conclusion, our experimental results clearly demonstrate YCrO_3 to be biferroic, with interesting magnetic properties. Our calculations support the observed ferroelectricity in YCrO_3 through the determination of the detailed structure. There are competing structural instabilities in YCrO_3 , and the dominating one is of anti-ferrodistortive type. Hence, the polarization found in YCrO_3 arising from the weak ferroelectric instability is relatively small. Our finding that the *G*-type AFM ordering is lower in energy than the uniform FM ordering is consistent with the experimentally known AFM phase of YCrO_3 and indicates that ferromagnetism in YCrO_3 can only be weak and its emergence at lower temperatures must be from mechanisms other than simple exchange type magnetic interactions, possibly canted AFM. It is possible that non-centrosymmetry in YCrO_3 is local in nature, an aspect that can be revealed by a study of the pair-distribution functions based on careful diffraction measurements. It appears likely that other chromites of heavier rare earths (Er, Ho, Yb, Lu) may also be biferroic.

Our preliminary measurements show that LuCrO_3 becomes ferromagnetic at 115 K (T_N) and ferroelectric at 488 K (T_E). Further studies are in progress, on these chromites.

The authors thank the Department of Science and Technology for support of this research. UVW thanks J. Bhattacharjee for help with xcrsden.

References:

- ¹N. A. Spaldin, *Physics world* April 2004, 20.
- ²N. A. Hill and A. Filippetti, *J. Mag. Mag. Mater.* **242-245**, 976 (2002).
- ³N. A. Hill, *J. Phys. Chem. B* **104**, 6694 (2000).
- ⁴T. Kimura, T. Goto, H. Shintani, K. Ishizaka, T. Arima and Y. Tokura *Nature* **426**, 55 (2003).
- ⁵A. Moreira dos Santos, A. K. Cheetham, T. Atou, Y. Syono, Y. Yamaguchi, K. Ohoyama, H. Chiba and C. N. R. Rao, *Phys. Rev. B* **66**, 064425 (2002).
- ⁶T. Kimura, S. Kawamoto, I. Yamada, M. Azuma, M. Takano and Y. Tokura, *Phys. Rev. B* **67**, R180401 (2003).
- ⁷I. Sosnowska, T. Peterlin-Neumaier and E Steichele, *J Phys C: Solid State Phys.* **15**, 4835 (1982).
- ⁸S. Niitaka, M. Azuma, M. Takano, E. Nishibori, M. Takata and M. Sakata, *Solid State Ionics* **172**, 557 (2004).
- ⁹M. Fiebig, Th. Lottermoser, Th. Lonkai, A. V. Goltsev and R. V. Pisarev, *J. Mag. Mag. Mater.* **290-291**, 883 (2005).
- ¹⁰Z. J. Huang, Y. Cao, Y. Y. Sun, Y. Y. Xue and C. W. Chu, *Phys. Rev. B* **56**, 2623 (1997).
- ¹¹G. V. Subba Rao, G. V. Chandrashekar and C. N. R. Rao, *Solid State Commun.* **6**, 177 (1968).
- ¹²L. Katz, *Acta cryst.* **8**, 121 (1955).
- ¹³V. M. Judin and A. B. Sherman, *Solid State Commun.* **4**, 661 (1966).
- ¹⁴T. Morishita and K. Tsushima, *Phys. Rev. B* **24**, 341 (1981).

- ¹⁵L. E. Cross, *Ferroelectrics* **151**, 305 (1987).
- ¹⁶L. E. Cross, *Ferroelectrics* **76**, 241 (1987).
- ¹⁷Q. Zhuang, M. P. Harmer, D. M. Smyth and R. E. Newnham *MRS Bull.* **22**, 1329 (1987).
- ¹⁸N. Uchida and T. Ikeda, *Jpn. J. Appl. Phys.* **4**, 867 (1965).
- ¹⁹S. Baroni, A. Dal Corso, S. de Gironcoli and P. Giannozzi, <http://www.pwscf.org>.
- ²⁰J. P. Perdew, J. A. Chevary, S. H. Vosko, K. A. Jackson, M. R. Pederson, D. J. Singh and C. Fiolhais, *Phys. Rev. B* **46**, 6671 (1992).
- ²¹D. Vanderbilt, *Phys. Rev. B* **41**, R7892 (1990).
- ²²H. J. Monkhorst and J. D. Pack, *Phys. Rev. B* **13**, 5188 (1976).
- ²³J. T. Looby and L. Katz, *J. Am. Chem. Soc.* **76**, 6029 (1954).
- ²⁴R. D. King-Smith and D. Vanderbilt, *Phys. Rev. B* **47**, R1651 (1993).
- ²⁵U. V. Waghmare and K. M. Rabe, *Phys. Rev. B* **55**, 6161 (1997).
- ²⁶A. Kokalj, *J. Mol. Graphics Modelling* **17**, 176 (1999).

Figure captions

- Fig. 1 Temperature-variations of magnetization of YCrO_3 (pellet). Inset shows magnetic hysteresis curves at different temperatures.
- Fig. 2 Temperature-variations of dielectric constant of YCrO_3 (a) pellet and (b) a thin film at different frequencies.
- Fig. 3 (a) Capacitance-voltage curves of YCrO_3 (b) dielectric hysteresis in YCrO_3 at different temperatures.
- Fig. 4 Structure of AFM YCrO_3 (8 formula units/cell): (a) structural distortions of the parent centrosymmetric structure are shown with arrows with lengths proportional to atomic displacements from the cubic structure, (b) cube-like surfaces surrounding Cr atoms are the isosurfaces of magnetization density at a value 10 % of its maximum. We have used XCRYSDEN software for visualization.²⁶
- Fig. 5 Density of electronic states with spin up (positive) and down (negative) near the energy gap of monoclinic structures with (a) antiferromagnetic and (b) ferromagnetic ordering.

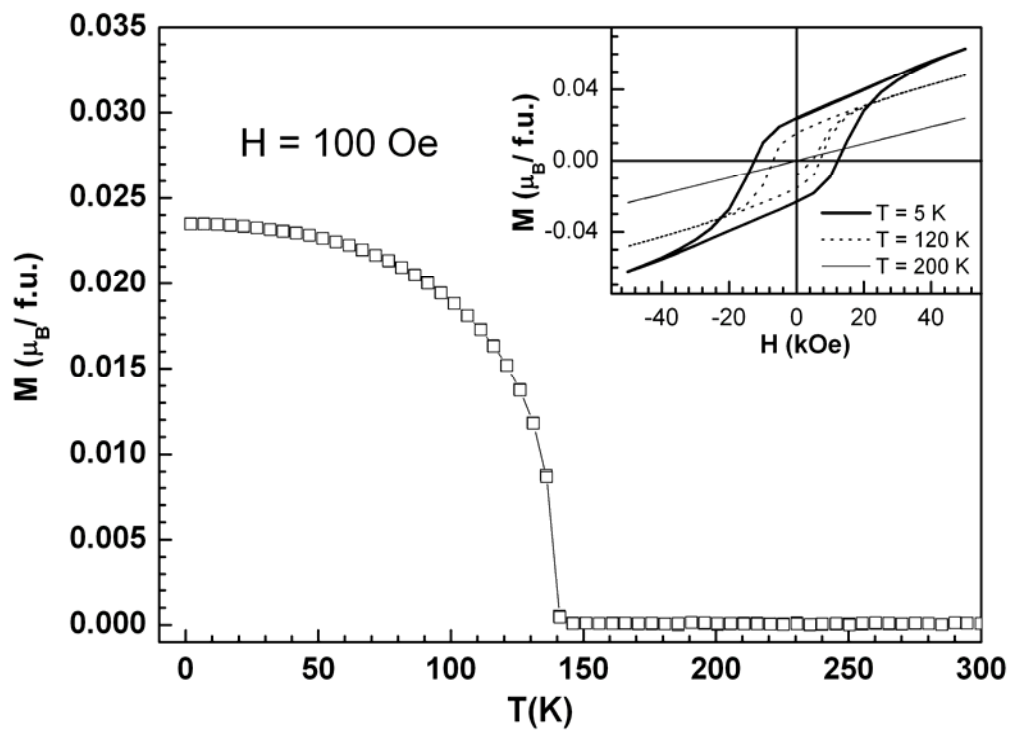


Fig. 1

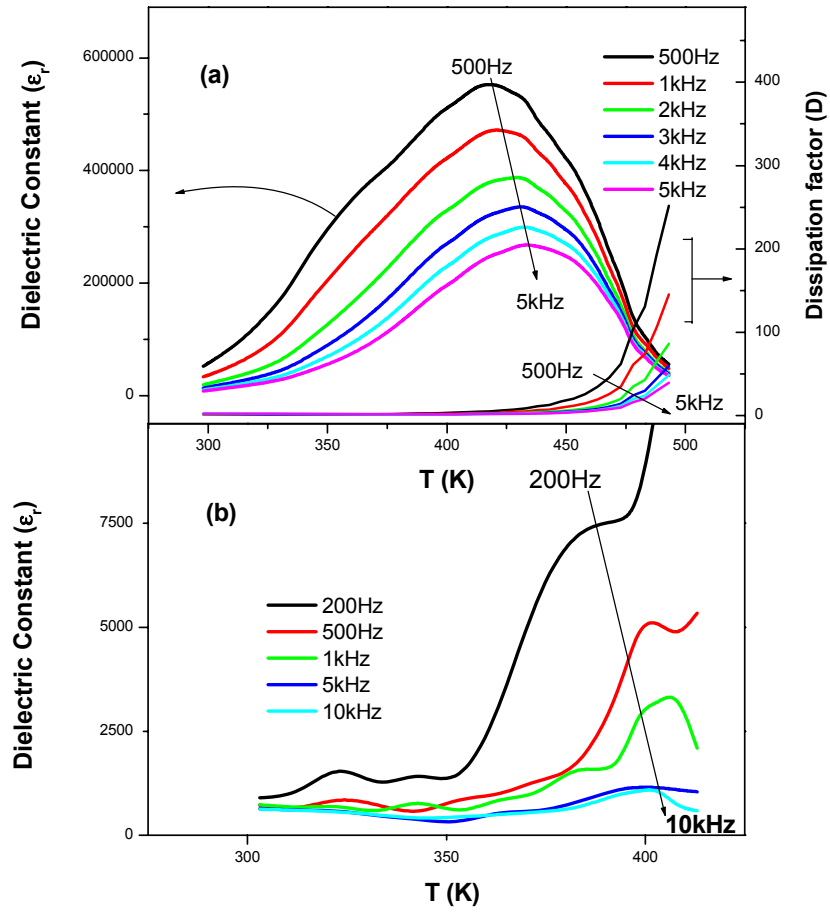


Fig. 2

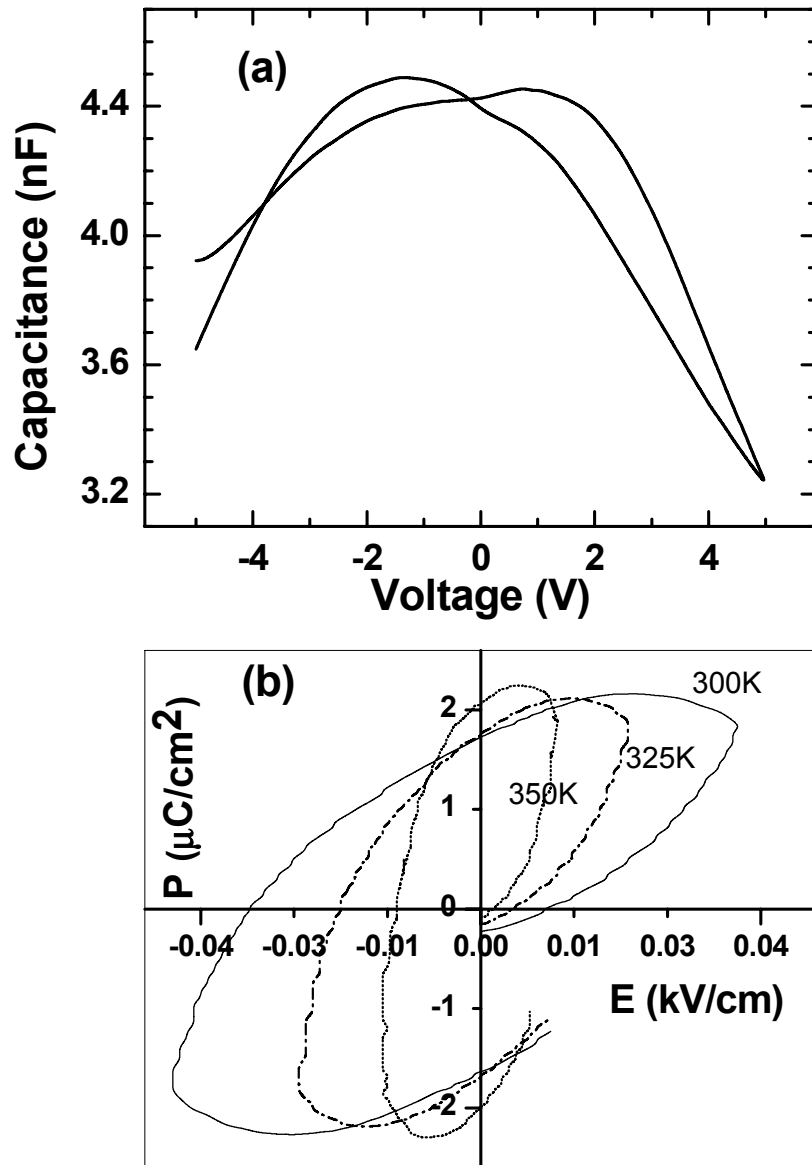


Fig. 3

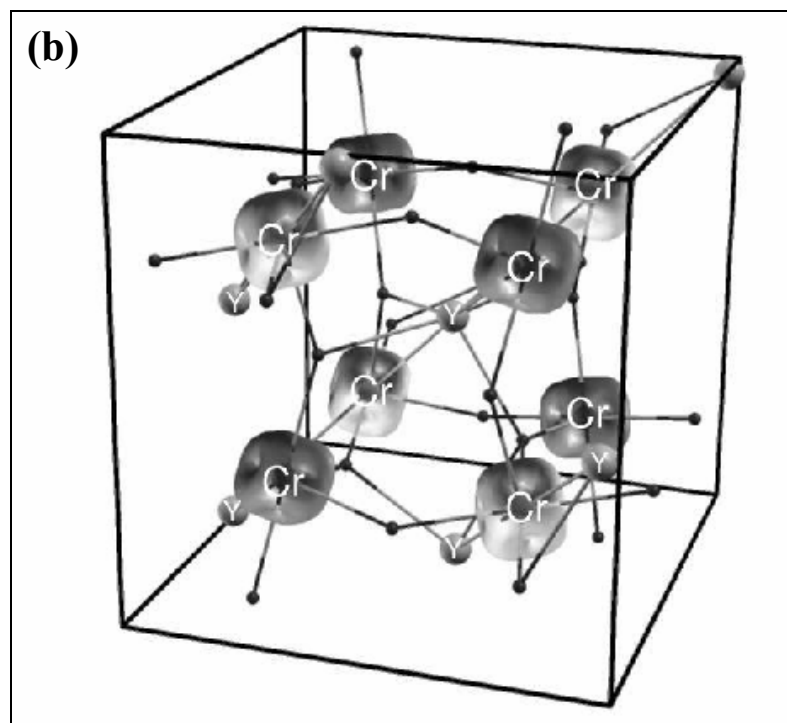
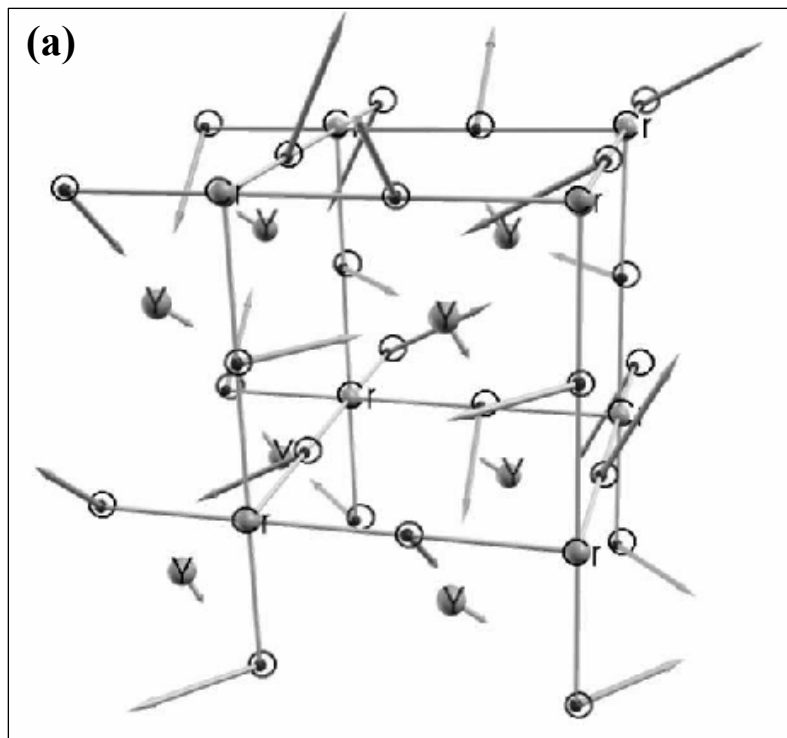


Fig. 4

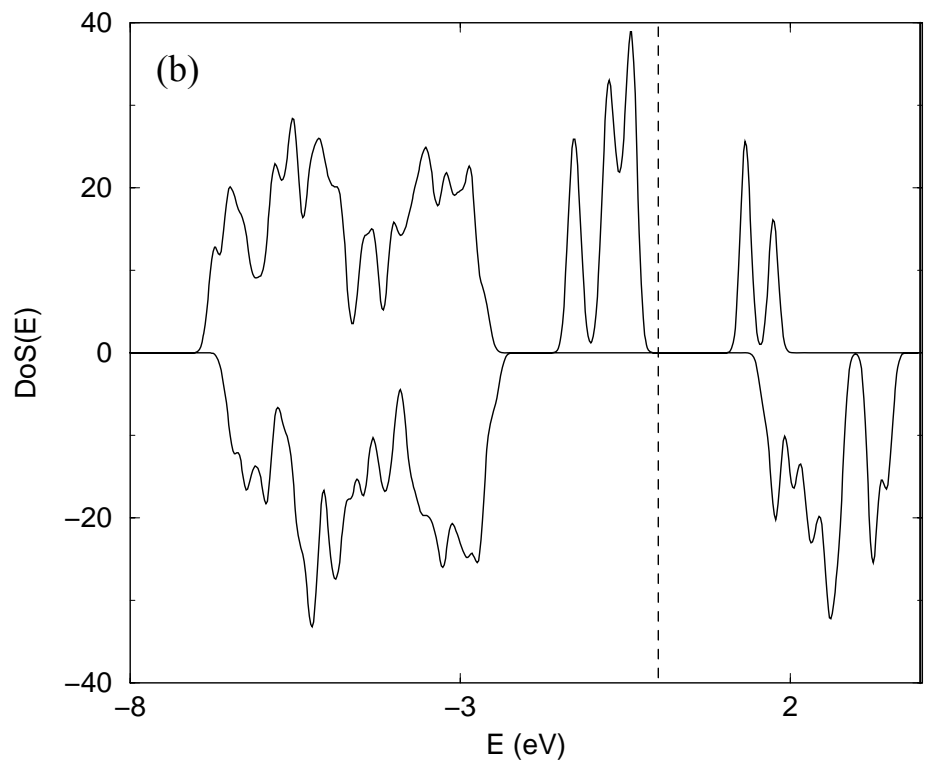
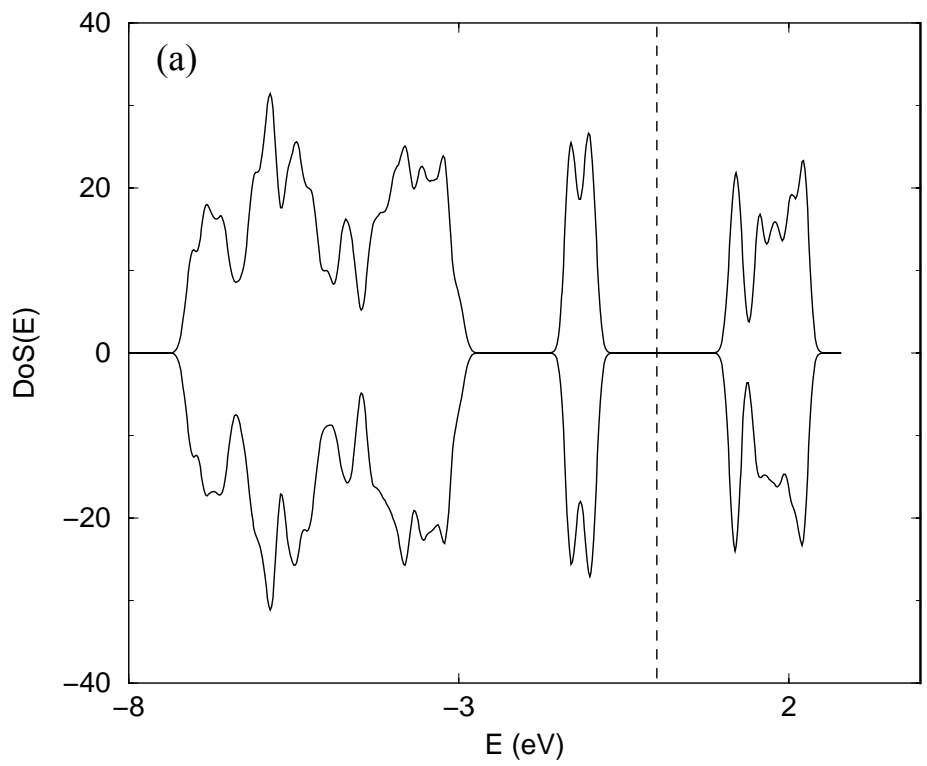


Fig. 5